

**Measurement Astrophysics and the AF Space Surveillance Mission**

**John T. McGraw, Mark R. Ackermann, Tom Williams,  
Peter C. Zimmer, Walter Gerstle, M. Suzanne Taylor, Jon Turner,  
Julie Smith, Justin Linford**  
*The University of New Mexico*

**G. Fritz Benedict, Stephen C. Odewahn**  
*The University of Texas at Austin*

**Lt. Col. Charles J. Wetterer**  
*US Air Force Academy*

**Gary G. Gimmestad**  
*Georgia Tech Research Institute*

**Victor L. Gamiz, Capt. David Frick**  
*AFRL/DE*

**Jeffrey R. Pier**  
*US Naval Observatory, Flagstaff*

**Charles F. Claver**  
*National Optical Astronomy Observatory*

**Dean C. Hines**  
*Space Science Institute*

**Jens Schwarz**  
*Sandia National Laboratories*

**and the Measurement Astrophysics (MAP) Research Group**

**ABSTRACT**

As part of the AFRL-funded Near Earth Space Surveillance Initiative (NESSI) the University of New Mexico's Measurement Astrophysics (MAP) Research Group has defined, designed and implemented several atmospheric measurement techniques to complement and supplement the observations of the CCD/Transit Instrument with Innovative Instrumentation (CTI-II). The principal idea driving the creation of atmospheric sensing and telescope metrology ancillary instrumentation is that these instruments produce data relevant to the reduction and analysis of astronomical data in the quest for quantitatively more precise and accurate photometric and astrometric observations of the night sky.

Instruments and techniques relevant to optical-infrared (OIR) space surveillance include:  
The Astronomical Lidar for Extinction (ALE) to measure precisely the time-dependent total atmospheric extinction  
A spectrophotometric telescope for measuring wavelength-dependent atmospheric extinction  
A differential microbarograph array to measure anomalous atmospheric refraction  
A multi-baseline microthermal array for measuring atmospheric turbulence on multiple spatial scales.

When implemented in support of the stationary, meridian-pointing CTI-II, designed to be the most precise ground-based photometric and astrometric telescope, these instruments operated together provide near real-time measurements of wavelength-dependent total atmospheric extinction caused by scattering and absorption by molecules and aerosols. They also characterize the time-dependent vertical atmospheric pressure and density above the telescope and measure the large-scale (degrees) tilt induced by atmospheric gravity waves, the apparent source of anomalous refraction.

Imaging, photometry and spectrophotometry of satellites can be dramatically enhanced by use of these low-cost deployable instruments. Applications relative to CTI-II will be described. The network of faint photometric and astrometric standard stars always observable in the northern hemisphere resulting from multi-year CTI-II observations and the utility of this network to sky surveys will be discussed and demonstrated.

## 1.0 MEASUREMENT ASTROPHYSICS

The terms “measurement science” and “measurement physics” are used to describe efforts to make precise and accurate physical measurements, typically involving new instrumentation, techniques, applications or algorithms. The American Physical Society includes a Topical Working Group on Instrument and Measurement Science with the objective of encouraging precision in measurements and supporting the development of instrument and measurement science.

Astronomy and astrophysics depend upon precise and accurate observational measurements to correctly describe the scale, motions and texture of the universe and the physical properties of all the objects it contains. We desire to bring the precision and accuracy supported by measurement science to observational astronomy and astrophysics. “Astrophysical accuracy,” implying measurement precision of perhaps a factor of two, is no longer acceptable in most observational programs. An important example is that the initial observational evidence for the accelerating universe and dark energy, upon which substantial research funding and effort is being invested, is that distant Type Ia supernovae appear systematically fainter than expected relative to expansion models, with a maximum deviation of only  $\sim 25\%$  at  $z \sim 0.7$ . The community requires and must demonstrate high precision and accuracy for high-value observations such as these.

Enhanced and continuously improving precision and accuracy clearly has a place in evolving astronomy, astrophysics and cosmology.

It can be argued that because of the wide variety and literal universality of the requisite measurements, nowhere is precision and accuracy more necessary to measurement than in astronomy and astrophysics. While the astronomical community has long sought precision for its often difficult observations, it is certain that continued development and application of precision measurement techniques will result in fundamental new physical understanding.

The essence of the scientific method requires a controlled experiment with repeatable results. This is usually arranged in physics by use of a laboratory or facility at which the identical experiment can be run multiple times. When the entire cosmos is the physics (or chemistry or biology) laboratory,

experimentation is not possible – science progresses on the basis of *observation*. In addition, the environment is not controllable because in a very real sense the environment we are sensing is the universe itself.

### **1.1 First Applications – Enhanced Accuracy Ground-Based Observations**

The environs of a ground-based telescope in which a great deal of observational error is created can, however, be controlled and the atmosphere intensively monitored. Our research group is first concentrating on capabilities to measure, monitor, control and correct for observational errors created by Earth’s atmosphere.

Proven, demonstrable observational precision and accuracy certainly leads to greater confidence when observing singular events. Many astrophysical phenomena, including supernova explosions, cannot be repeated, thus a premium accrues to observations where repeated observations of known “standard” stars ensures precision and full control of the observational uncertainties of all observations, including unique and singular events. A proven standard field of stars, calibrated for astrometry and photometry, would help the astronomical community immensely.

### **1.2 An Example of Measurement Astrophysics**

The UNM Measurement Astrophysics (MAP) Research Group is undertaking a program to define instruments and techniques to achieve space-based precision in photometry and astrometry with ground-based telescopes. These techniques and instruments are designed to be applicable at observatories worldwide, to be cost-effective to implement and to be fundamentally simple.

For decades ground-based optical-infrared (OIR) astronomical observations have been affected by a host of physical effects associated with the time-dependent transmission, scattering and refraction by Earth’s atmosphere. These effects have limited terrestrial OIR images to ~ 1% - 2% photometry and ~ 0.01 arcsecond astrometry. Additionally, current practices for correcting the instrumental signature and photometric and radiometric calibration have not been as accurate as they could be. Typically, astrometric and photometric results have often been worse than errors derived from photon and detector noise statistics because of uncorrected – or even undetected – systematic errors.

A practical example involves photometry in optical bandpasses. For this example we discuss terrestrial effects on area-format imaging observations.

#### ***Time-Dependent Atmospheric Extinction Corrections – An Example***

As light from a star passes through Earth’s atmosphere some of that light is lost to absorption and scattering. That light loss is referred to by astronomers as “extinction.” It is wavelength dependent, with blue light losses greater than for red light, and it depends upon the optical path length through the atmosphere with greater losses incurred at greater zenith distance (equivalently lower angular altitude or longer path length).

The light from a star is measured as an *intensity*, that is, as a number of detected photons per second. The application of the correction for light lost to extinction usually occurs after converting the measured intensity to an *instrumental magnitude*  $m_I$  :

$$m_I = -2.5 \log_{10} I_{obs} + m_0$$

where  $I_{obs}$  is the observed intensity and  $m_0$  is the zero-point of the instrumental magnitude system. The correction for atmospheric extinction is applied to this instrumental magnitude and results in a magnitude that would be measured were there no intervening atmosphere, that is, as though the measurement were made from space. The formalism for extinction typically assumes a

unitary “airmass” at the zenith – straight above the observatory there is one standard atmosphere corrected for the altitude of the observatory. At larger zenith distance the airmass and the path length through the atmosphere increases, resulting in additional extinction. The procedure is to calibrate the extinction per airmass and then multiply by the normalized airmass (path length) at the zenith distance of the observation. The existing formalism is:

$$m = m_1 - A(\lambda, \Delta\lambda)M(z)$$

where  $A$  is the “extinction coefficient” in units of magnitudes per airmass, and  $M$  is the airmass in the direction of the star.

Astronomers typically measure  $A$  by observing a set of stars having a range of color at different times during the night - that is, at a series of airmasses. The slope of the plot of magnitude vs. airmass estimates the extinction coefficient for the night, and stars of differing color provide the wavelength dependence of the extinction. Because observing extinction stars subtracts from observing time on program stars, extinction measures are typically made only a few times per night. A usual procedure is to combine extinction measurements from all observers at an observatory to produce seasonal or monthly mean extinction coefficients. While this results in a well-defined mean, the variance of this mean can be large and is certainly time dependent on scales as short as minutes. In fact, common experience of watching the sky confirms that formation and motion of clouds, lifting of dust, propagation of smoke and aerosols all happen on timescales of minutes. It is reasonable to infer that nighttime extinction changes can happen on that same timescale, and thus significant extinction variations can occur in the course of a single integrated observation, and certainly during the course of a night. Classical techniques for measuring extinction do not sample in the time domain sufficiently often to detect, measure and monitor these extinction variations.

We thus explicitly write  $A = A(\lambda, \Delta\lambda, t)$  as a function of time. Additionally,  $A$  is a function of the wavelength,  $\lambda$ , at which the coefficient is applied, as well as the bandpass,  $\Delta\lambda$ , over which it is applied. Neither the time nor the bandpass dependence of the extinction coefficient is usually recognized.

We also write  $M = M(z, t)$  because the airmass is certainly a function of the zenith distance, but less recognized, the airmass itself is also time dependent on timescales of hours, the time scale of frontal motions. Thus, even the zenith airmass is a function of time.

Our formalism for more accurate time dependent extinction corrections is thus:

$$m = m_1 - A(\lambda, \Delta\lambda, t)M(z, t).$$

Note that an error in correcting for extinction limits the precision of the resulting corrected magnitude to (at least) this same error. Thus, a 1% error in the extinction correction, from any source, can result in a 1%, or 0.01 magnitude, error in the observed magnitude corrected to outside Earth’s atmosphere.

The quest for precision ground-based photometry requires that atmospheric extinction corrections be measured as precisely as the program stars.

Because of the time dependence of extinction, it must be measured at the same time and on the same time scale as observations of the program star. New instrumentation and techniques are required to accomplish extinction measurements that will enable more precise and accurate photometry.

## 2.0 THE CCD/TRANSIT INSTRUMENT WITH INNOVATIVE INSTRUMENTATION (CTI-II)

A survey telescope that remains fixed in the meridian near the zenith while accomplishing a multi-year synoptic survey leads to reproducible high precision photometric and astrometric observations. Gravity loading on the fixed telescope remains constant with time, and the airmass is minimized and constant because of near zenith pointing. These are observing conditions favorable to precision astronomical observations, and to the application of measurement astrophysical techniques to the survey. In addition to a high precision synoptic survey of the sky, a significant product of the CTI-II survey will be a photometric and astrometric catalog of radiometric and positional “standard stars.”

The CCD/Transit Instrument with Innovative Instrumentation (CTI-II) is the second iteration of the original CCD/Transit Instrument (CTI) built and operated on Kitt Peak from 1984 until 1992 [1-4]. CTI was a unique, stationary transit telescope that observed in the meridian, repeatedly observing a small circle on the sky at a declination of  $+28^\circ$  with nightly cadence. CTI used the time-delay and integrate (TDI or “pushbroom”) continuous readout technique at the sidereal rate as schematically depicted in Fig. 1. While CTI-II will operate in the same mode, and indeed include the original surveyed strip as a subset of its field of regard, there are highly significant differences between the two implementations. Whereas the original CTI used two early RCA CCDs with  $512 \times 320$  30micron pixels to survey an 8.25arcmin wide strip of the sky in two bandpasses, CTI-II will use a mosaic of approximately 40 CCDs to observe a fully-corrected one degree wide swath of sky in five bandpasses. CTI produced an (at the time) astonishing 450 Mbytes of image data every clear night, whereas CTI-II will produce a (now) modest 450 Gbytes of data per night. The large RCA pixels undersampled the Kitt Peak seeing blurred PSF and added 45 electrons of readout noise per pixel. The 60 micron/arcsec field scale of CTI-II will put at least 2.2 20 micron pixels with 5 electrons of readout noise per pixel across the FWHM of a 0.7 arcsec seeing disk, resulting in a much better sampled seeing-blurred PSF and a higher signal-to-noise ratio (S/N) image. CTI-II is being sited at McDonald Observatory in West Texas, where the seeing has been measured to be 0.7 arcsec or better for about 10% of the available observing time.

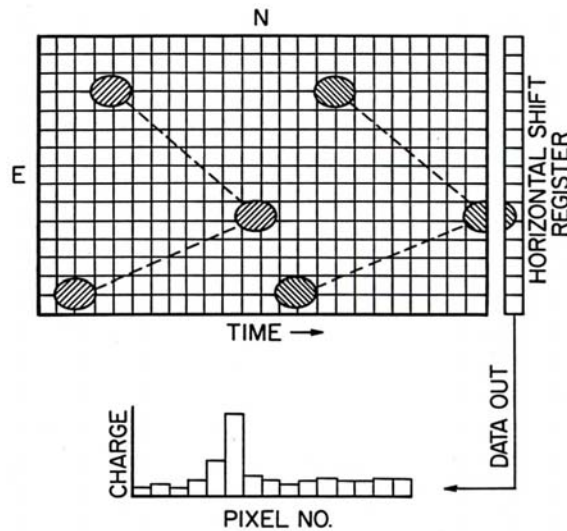


Fig. 1. Schematic description of the time-delay and integrate (TDI) mode of CCD operation. As the sky transits the CCD, the charge image is shifted at the sidereal rate to keep it below the optical image. The charge image is thus integrated in the CCD for the time required for the field to transit the device. As the image reaches the horizontal shift register, it is serially read out, digitized and stored in memory. Individual star images are shown elongated along CCD columns to represent the  $\sim 1/2$  pixel blur induced by discretely shifting the charge image beneath the continuously moving optical image.

CTI was the first instance of implementation of several designs and techniques used or planned for other telescopes. The Sloan Digital Sky Survey (SDSS) [5], the Palomar-Quest Survey [6], the Flagstaff Astrometric Scanning Transit Telescope (FASTT) [7] and the Carlsberg Meridian Telescope [8] all adopted the TDI CCD readout technique. The Large Synoptic Survey Telescope (LSST) uses a modified Paul-Baker optical design [9] first used on the sky by CTI [3].

CTI-II is being designed and implemented at McDonald Observatory where a site survey has been completed and a site on the southwest ridge of Mt. Locke has been selected. This site has favorable seeing and wind conditions and will support the precision astrometric and photometric observing program of CTI-II. In addition, of the two finally contending sites, the southwest ridge of Mt. Locke has the better developed infrastructure. The CTI-II site is shown in Fig. 2.



Fig. 2. The CTI-II site on the southwest ridgeline of Mt. Locke. The site is favorably located into the prevailing winds and takes advantage of relative orographic isolation both from topology and from other buildings and structures.

Site testing included seeing monitored with Differential Image Motion Monitors (DIMMs), microthermal profiles to 12 meters above grade, wind direction and speed, free air temperature, relative humidity, frequency of lightning strikes and subsurface integrity. On these bases the CTI-II site on Mt. Locke was selected.

The optical design, the layout for which is shown in Fig. 3, is a unique “bent Cassegrain” system that has been shown to be generally useful to astronomers [10]. The design has been finalized, a sensitivity analysis has been analyzed, ghosting has been investigated and shown to be negligible, and baffling designs have been investigated. Fabrication of the reflective secondary and tertiary (flat) mirrors and the five lens, all-spherical refractive corrector will commence shortly.

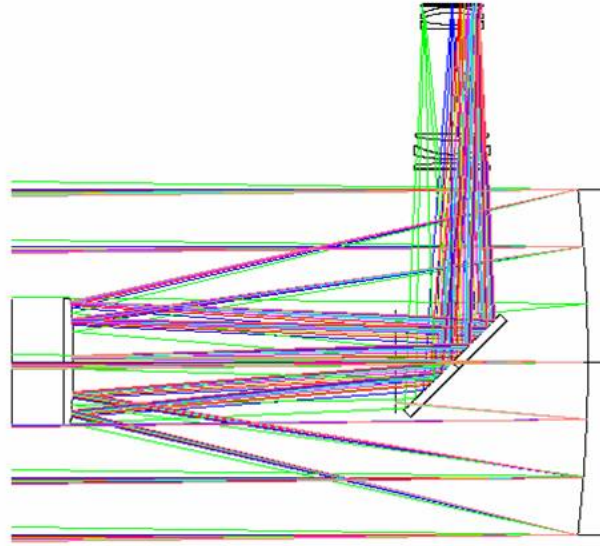


Fig. 3. The layout for the CTI-II bent Cassegrain optical system. This optical system produces a 1.4degree FOV with a field scale of 60 microns/arcsec, with near diffraction limited images from 400nm to 1100nm, and with 0.001% full-field distortion. Colored rays encode off-axis angle defining the FOV.

A unique thermally compensating optical support structure (OSS) has been designed using carbon fiber epoxy (CFE) composites. This rigid, low thermal mass structure has a lowest resonant frequency at 30 Hz. The thermal expansion coefficients of various CFE substructures have been designed to make the structure virtually insensitive to diurnal thermal variations, making it unnecessary to actively focus the telescope. The structural layout is shown in Fig. 4.

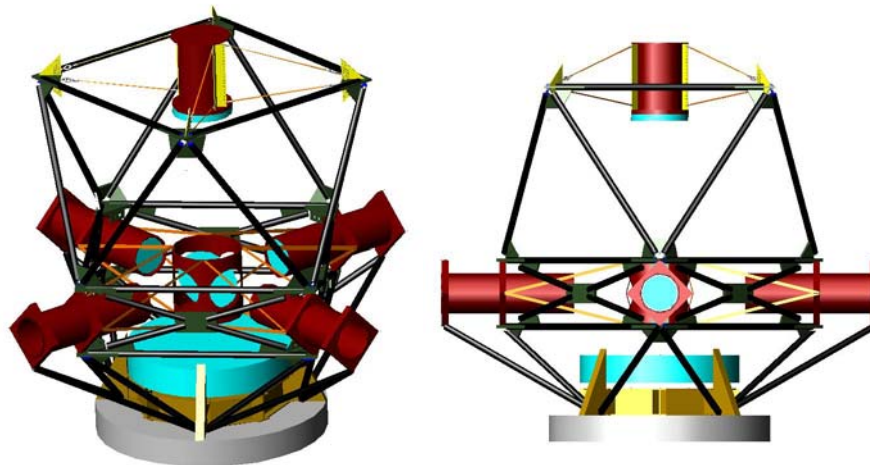


Fig. 4. The carbon fiber epoxy (CFE) optical support structure (OSS) for CTI-II. The 3-D view (left) shows cross sections supporting the primary, secondary and tertiary mirrors. The primary mirror is 1.8m in diameter. Four port structures are show. The port fed by the tertiary mirror contains the CCD camera. A cross sectional view is shown at the right.

Site testing shows that elevating CTI-II higher than nine meters above the ground significantly improves seeing quality. A pier and enclosure will place the telescope 10m above grade. The simple enclosure is designed as the exoskeleton of the telescope. It provides environmental protection but contains little thermal mass and has controlled emissivity surfaces to minimize the onset of convection from the telescope surroundings. The enclosure provides free air flow around the telescope. The goal is to control the temperature of the telescope and match it quickly to the free air temperature thus preventing the onset of convective heat transport, which locally degrades the seeing. The enclosure is shown in Fig. 5.

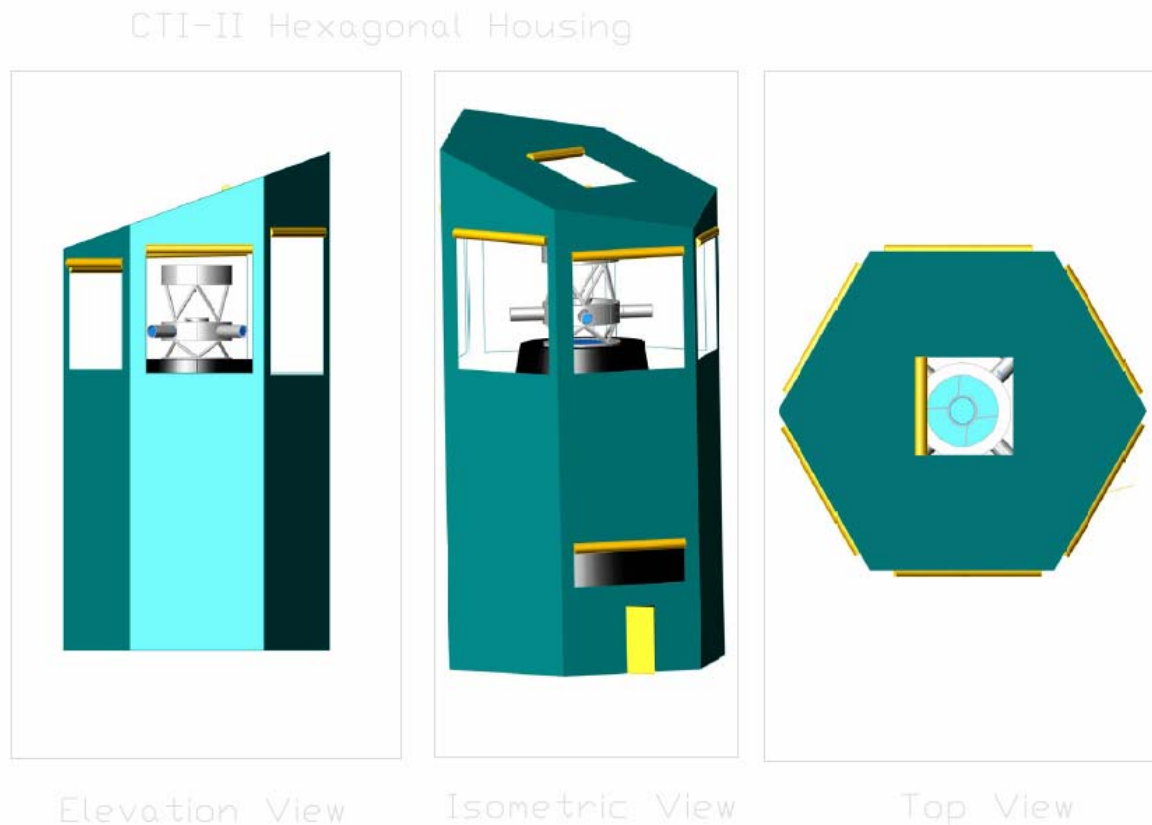


Fig. 5. The hexagonal exoskeleton of the CTI-II. The telescope is mounted on a rigid pier 10 m above grade. The lightweight building protects the telescope and pier from direct solar illumination during the day, but opens up to ventilate and cool the telescope to the near the free air temperature at dusk, thus obviating local or “dome seeing.” The enclosure is constructed of low thermal mass materials and radiating surfaces act to control the thermal environment. An absolute minimum of power sources are housed in the enclosure. The control and data computer systems are housed in a separate building to the north, normally downwind of the telescope enclosure.

### 3.0 OBTAINING EARTH’S EVIL ATMOSPHERE

While Earth’s atmosphere isn’t truly *evil*, it does negatively perturb ground-based astronomical observations.

Our atmosphere transmits a fraction of the electromagnetic spectrum, but that fraction contains valuable astrophysical information and deserves to be measured with the utmost precision and accuracy. We can’t significantly change the transmission of the atmosphere, in any event. Earth’s atmosphere is a turbid

refractive optical medium that attenuates transmitted radiation. It also is a scattering medium and is an optical element with a spatially variable index of refraction. Further, it supports optical turbulence that moves and blurs images.

In addition, each of these effects is time-variable on timescales ranging from milliseconds to years. Certainly most of these effects change on timescales shorter than a typical astronomical observation. UNM's Measurement Astrophysics (MAP) Research Group realized that astronomers are not using all available information, principally derived from atmospheric physics measurements, to correct for atmospheric effects. These include total astronomical extinction and large-scale refractive displacements - "anomalous refraction" - and other effects that have plagued ground-based observations for centuries. Of course, the "noise" introduced into astronomical observations by the atmosphere is largely "data" for atmospheric scientists.

Our efforts are directed at obviating the deleterious effects on astronomical observations induced by the atmosphere by making relevant physical measurements of Earth's atmosphere in parallel with astronomical observations. We thus describe current efforts to define new instruments for observatory use, including the NSF-funded Astronomical Lidar for Extinction (ALE), absolute spectrophotometric calibration to obtain wavelength-dependent extinction, differential microbarograph arrays for measuring coherent (gravity mode) atmospheric wave structure, and microthermal arrays for assessing turbulent structure in the vicinity of the telescope - all acquired with high temporal resolution simultaneously with astronomical observations.

The driver for these MAP efforts is the goal of approaching space-based photometric and astrometric observations with the stationary CTI-II.

### **3.1 The Astronomical Lidar for Extinction (ALE)**

The Astronomical Lidar for Extinction [11, 12] provides two primary measurements of the atmosphere useful for photometry and astrometry. The most familiar is the measurement of total atmospheric extinction. The second is measuring  $\sim 10 - 60$  minute timescale quasi-periodic refractive changes that produce an effect known historically as *anomalous refraction*.

Anyone who observes Earth's atmosphere - or flies through it - knows that transparency and turbulence change on timescales ranging from minutes to days. Historically, the corrections to astronomical observations for absorption and scattering in the atmosphere, *astronomical extinction*, have been done by using extinction coefficients derived by "averaging" over a night, a month, or in some cases, a season. Our common sense based upon looking at the sky indicates that while one can establish a well-defined mean extinction over a long timescale, the variance must be large because of the much shorter timescales on which we know that extinction can and does change. The timescales for formation and motion of clouds is an example. ALE is designed to measure total atmospheric extinction with a cadence of one minute in the direction of observation to allow calculation of precise and accurate extinction that actually applies to each observation.

The eye-safe ALE is designed to provide lidar ranging to 90 km. It incorporates a pulsed laser transmitter, a short-range and a long-range receiver.

The transmitter is a separate optical system from the receivers. It is a 317.5-mm diameter off-axis spherical system mounted on the side of the long-range receiver. The diameter is required to maintain eye safe operation using the Photonics Industries DC10-527 laser selected to replace the originally proposed microchip laser. The Nd:YLF Photonics DC10-527 operates at 526.5 nm with a variable pulse repetition rate up to 10 kHz. It produces a pulse energy of 100  $\mu$ J per pulse at 1500 Hz, the nominal pulse repetition rate specified for ALE.

ALE uses a short- and a long-range receiver to maintain the largest possible return pulse detection dynamic range, which ensures the greatest span of range bins. The short-range receiver provides range bins from

about 100 m to about 2 km. The long-range receiver provides range bins from about 2 km to 60 km or greater.

The short-range receiver is a 100-mm diameter, 800-mm EFL refractive telescope. The detector optics, and the detector itself, are identical to those used in the long-range receiver.

The long-range receiver is based on a 673-mm diameter Richey-Chrétien reflecting telescope. It is named the Flint Telescope in honor of the designer and donor of this very robust telescope. The Flint Telescope is being refurbished with new secondary mirror mount and stepper motor driven altitude and azimuth drives.

The detector for each channel is a photomultiplier tube (PMT). Pulses from each tube are measured in current measurement mode to accommodate high pulse return rates. Each channel incorporates a high efficiency, 20 nm wide bandpass filter to exclude moonlight, night sky emission, light pollution, and to minimize the effect of stars that happen to appear in the pupil aperture. A field lens and a Fabry lens image the pupil of each receiver onto its PMT.

ALE is designed to provide a million detected photons per minute returned from altitudes above 20km from Rayleigh (molecular) scattering alone. ALE is thus most effective when the atmosphere is relatively clear and astronomical observations are taking place. The data from ALE will provide a real-time total extinction measurement at 527 nm every minute of time. This provides a transmissivity record from which extinction measures can be calculated and applied to an integrated observation accurately representing the actual extinction of the atmosphere during each observation.

Modeling of ALE returns under representative conditions supports the claim that ALE will be both diagnostic of atmospheric conditions and quantitatively measure the total atmospheric extinction. Fig. 6 shows a simulated lidar return from a cirrostratus layer at about 10km altitude with the return profile dominated by Rayleigh scattering. The return plot includes Poisson noise and is digitized to simulate the operational ALE.

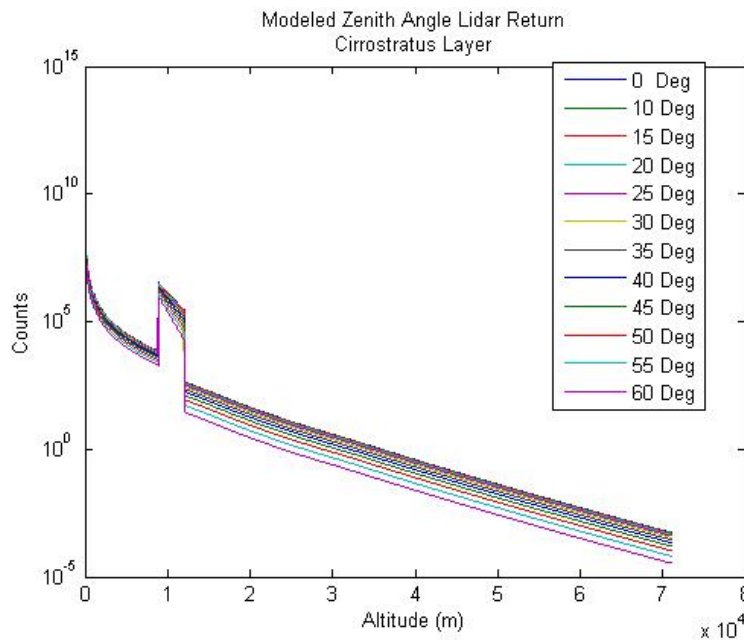


Fig. 6. Model ALE returns integrated for 60 seconds at 2500 pulses per second and parameterized by zenith angle for a pure Rayleigh atmosphere that includes a uniform cirrostratus layer at 10km altitude. These returns are not range corrected.

### 3.2 Astronomical Extinction Spectrophotometer (AESoP)

While ALE provides an accurate time-resolved total extinction measurement, it does so at the laser wavelength of 527nm. Atmospheric extinction is wavelength dependent, thus we are designing and testing the Astronomical Extinction Absolute Spectrophotometer (AESoP). AESoP is based upon a small telescope that obtains spectra of bright ( $V < 5$  magnitudes) spectrophotometric standard stars as they transit the meridian, close to the zenith, the field of regard of CTI-II, and the direction in which ALE measures monochromatic extinction. The AESoP spectra can be calibrated at 527 nm by the ALE extinction observations. The spectra then provide the wavelength dependence of extinction derived from comparing the observed to the standard spectra for each star.

AESoP measures a spectrum with signal-to-noise better than 100 per resolution element every minute of time. The combination of AESoP and ALE data allow accurate time- and wavelength-resolved extinction measurements to be applied to each of the five bandpasses observed by CTI-II.

In order to minimally perturb the instrumental signature of the bright star spectra, and because the required spectrophotometric resolution is low (approximately 10 nm) colored glass filters, commonly used for laboratory spectrophotometric wavelength calibration, are being investigated for use with AESoP. Fig. 7 shows a model spectrum for the primary astronomical spectrophotometric standard star Vega (top), and the spectrum with a holmium (middle) and didymium (bottom) filter response imposed on the stellar spectrum.

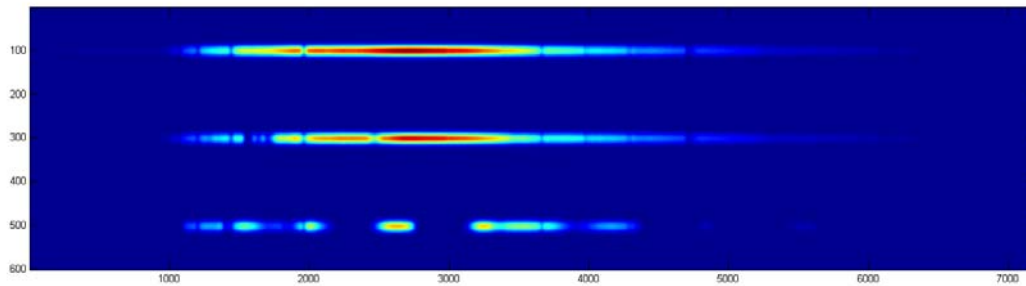


Fig. 7. Model spectra for Vega with absorptive wavelength standards superimposed. The top spectrum is for the bright ( $V = +0.03$ ) primary spectrophotometric standard star Vega with spectral type A0 V. The middle spectrum represents the spectrum of Vega observed with a holmium filter in the beam, and the lower spectrum shows the result of inserting a didymium filter on the spectrum.

### 3.3 Microbarograph Array for Anomalous Refraction (MuBAR)

Anomalous refraction (AR) has been with astronomers for more than a century, but the use of imaging telescopes incorporating time-delay and integrate (TDI) readout modes has brought this atmospheric effect to the fore. AR can be described as a wavefront tilt causing positional displacements of  $0.001 - 0.1$  arcsec over fields of view of degrees, with quasi-periodic time dependence of minutes.

AR has been attributed to atmospheric gravity waves, a phenomenon well known to atmospheric physicists. In the field of astrophysics on the other hand, while the atmosphere is well known as the prime limiting factor in ground based imaging capabilities, atmospheric gravity waves and their major dynamical influence on the atmosphere are virtually unheard of. These waves and their possible refractive modulations of astronomical images have been acknowledged in only a small handful of papers spread over more than a century. Despite their astronomical obscurity, atmospheric gravity waves may be one of the largest consistent sources of error in ground-based astrometric measurements.

The most detailed exploration of anomalous refraction in the current era was done by Pier, *et al.* [13]. Pier noted quasi-periodic residuals when comparing stellar positions determined by the Sloan Digital Sky Survey (SDSS) with those of the US Naval Observatory CCD Astrograph Catalog (UCAC) and Tycho2 astrometric catalogs. These residuals were described as having peak-to-peak amplitudes of several tenths of an arcsecond and quasi-periods of a few to several tens of minutes. Comparison of residuals from each of the CCDs in the focal plane array showed a high degree of consistency across the 2.3° array, indicating that the motion is due to atmospheric distortions which are coherent over at least this scale on the sky. Pier suggests that the source of the observed refractions may be atmospheric gravity waves occurring at altitudes of a few hundred meters up to 2 km. A schematic model for anomalous refraction created by an atmospheric gravity-mode wave is shown on Fig. 8.

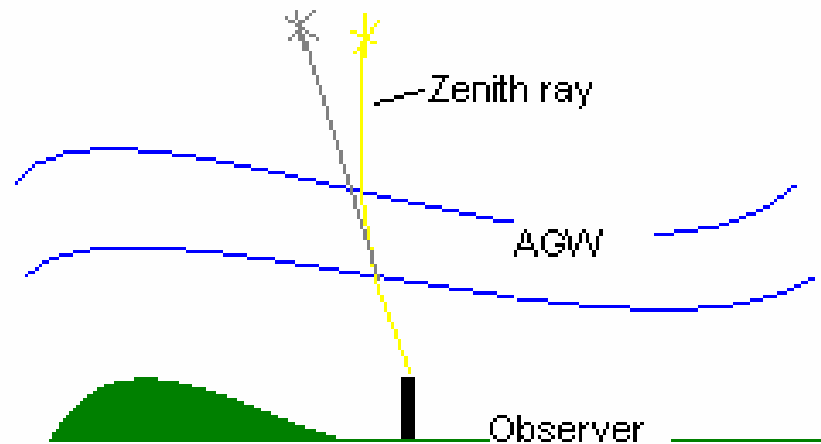


Fig. 8. A schematic atmospheric gravity wave (AGW) will refractively displace the apparent position of stars, and the displacement will change as the wave propagates. Displacements of 0.1 arcsec or larger over fields of view greater than 2.3 degrees have been measured. The displacements are quasi-periodic with representative periods of 10 – 60 minutes. Anomalous refraction induced by gravity waves can be a significant effect for astrometry, especially for large field astrometry with rapid cadence.

To characterize the presence and passage of atmospheric gravity waves, we have developed a differential microbarograph array. Based upon commercially available differential pressure sensors, these differential pressure detectors are sensitive at the 1 – 100 microbar level. Several differential arms can be deployed with different orientations and spacings to create a fully sampled “image” of the atmospheric pressure above an observing site. Fig. 9 shows UNM graduate student M. Suzanne Taylor testing a single differential microbarograph arm on the UNM Physics and Astronomy Department roof.



Fig. 9. UNM graduate student M. Suzanne Taylor tests a microbarograph array element. The differential atmospheric pressure between the two open ends of the 10 m element is measured by a sensitive differential pressure sensor in the middle box immediately in front of Suzanne. Each end of the element has baffling to preclude saturating the sensor on wind-induced noise. The pressure sensor is read at a 10Hz rate under control of LabVIEW.

### **3.4 Microthermal Array for Atmospheric Turbulence (MuTE)**

The local atmosphere can dominate the astronomical seeing experienced by a telescope. While CTI-II and its enclosure are designed to obviate convection, the optical turbulence convection creates, and resulting degraded seeing, the forces potentially acting to create atmospheric turbulence are many and almost impossible to predict based upon additional local factors such as temperature, wind speed and direction. The telescope itself measures the seeing as the full width at half maximum of the seeing-blurred point spread function. To counter local effects, we must know their amplitude and the scale of their effect. The appropriate technique is to measure the spectrum of atmospheric turbulence at the telescope. Something can usually be done about local effects if they are detected. Other than installing adaptive optics (AO), little can be done about seeing generated at altitude. CTI-II will not include AO, but will strive to improve (or at least not generate) observatory-scale turbulence.

Optical turbulence is produced by volumes of air at slightly different temperatures, thus different indices of refraction, crossing the optical path of the telescope. We've thus designed and built a prototype microthermal sensor system, the MicroThermal Experiment (MuTE), to measure the spectrum of atmospheric turbulence at a one minute (or faster) cadence. MuTE samples microthermal probes at one kHz to form a pair-wise variance of the temperature fluctuations across each of the 36 independent baselines created by nine probes. The power spectrum of atmospheric turbulence over the set of spatial frequencies can be directly calculated, as shown in Fig. 10.

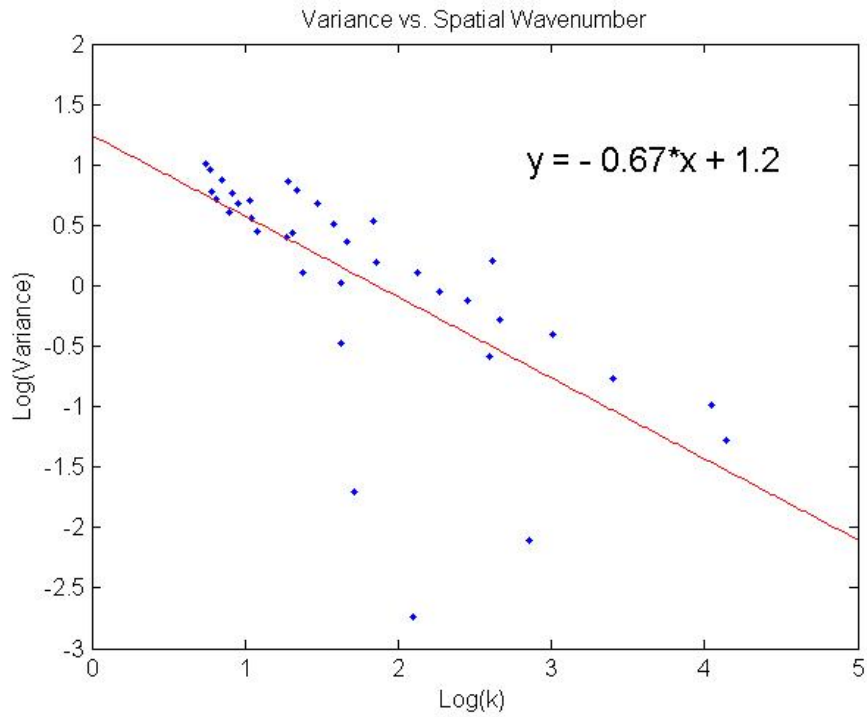


Fig. 10. Spatial power spectrum of the microthermal atmospheric fluctuations measured at 1430 on 18 July 2007 at the UNM Campus Observatory, 3m above grade, averaged over one minute. The linear regression in the log variance – log wavenumber plot has a slope of approximately 2/3, the value expected from Kolmogorov turbulence theory [14, 15].

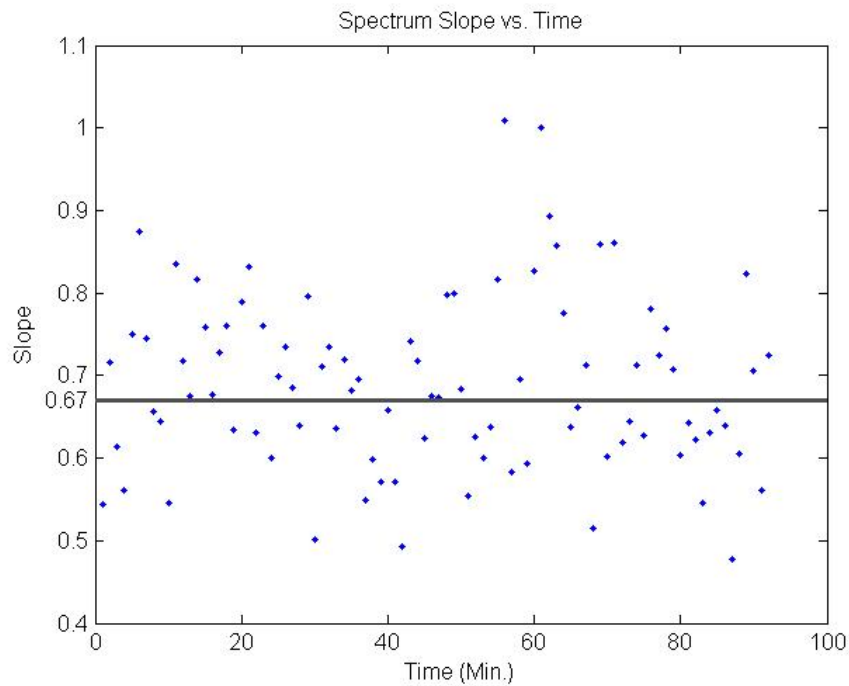


Fig. 11. The spectral slope as a function of time showing additional one minute intervals similar to that shown in Fig. 10. The expected slope of 0.67 is shown for reference.

The MuTE is undergoing modification to lower the instrumental noise and to make the instrument more robust. The goal of MuTE is to measure the spectrum and outer scale,  $L_0$ , of the atmosphere actually affecting the telescope.

#### 4.0 THE NORTHERN HEMISPHERE STANDARD STAR STRIP

A data product of potentially great value to the AF space surveillance mission that derives from CTI-II observations is a northern hemisphere catalog of “standard stars” to faint limiting magnitude. This strip, which will contain thousands of photometric and astrometric standard stars, will be useful for radiometric calibration of space-based as well as ground-based observations. The calibration will have well established uncertainties that have been established by observations repeated daily for several years and annually for several years. Our goal is to provide this strip with calibrations from which “the usual” deleterious effects of Earth’s atmosphere have been measured, modeled, calibrated and removed from the astronomical observations. We intend this to be the most precise and accurate, high confidence set of standard stars ever produced, and the precision will be proven and documented by the dense repeated set of observations.

The density of stars observed by CTI-II will be a function of the Galactic latitude and longitude of the field. Fig. 12 shows an infrared view of the Milky Way from the 2MASS short wavelength observations. This image, a “self portrait of the Milky Way,” indicates the Galactic coordinate system and shows the decidedly non-uniform distribution of stars.

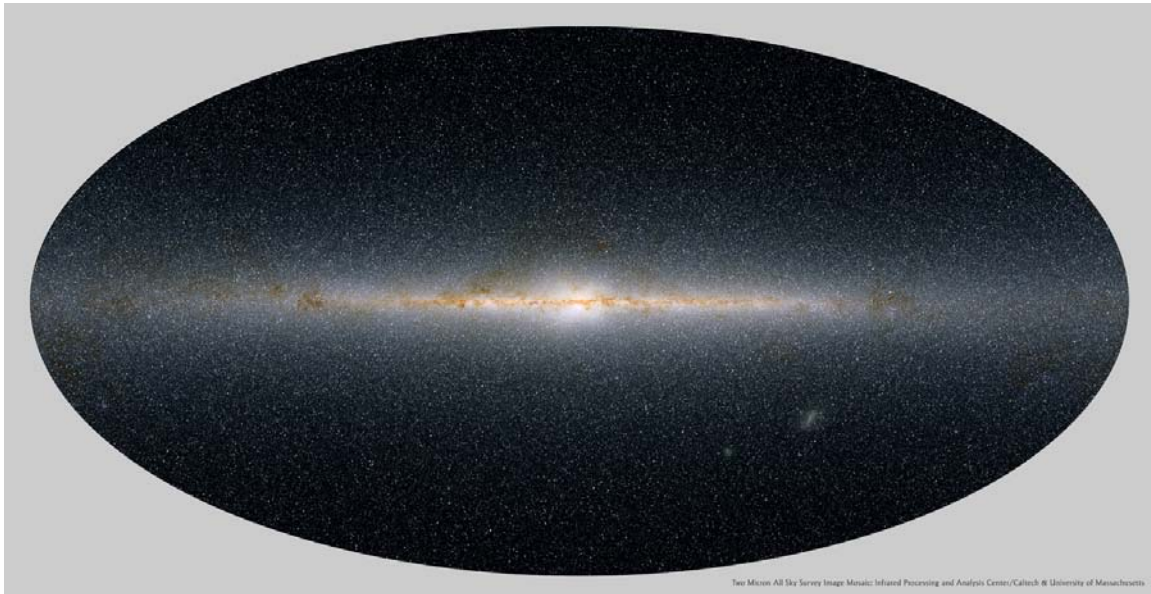


Fig. 12. The distribution of stars in the Milky Way. This image derives from 2MASS short wavelength observations with blue indicating 1.2 micron measurements, and green and red representing 1.6 and 2.2 micron observations, respectively. The observations represent the distribution of stars in the Milky Way, with the red stars in the plane of the Galaxy obscured and reddened by interstellar dust, which is concentrated in the Galactic plane.

Fig. 13 shows the CTI-II field of regard in Galactic coordinates (left) and in equatorial coordinates (right), which shows the field of regard as it will be observed at constant declination.

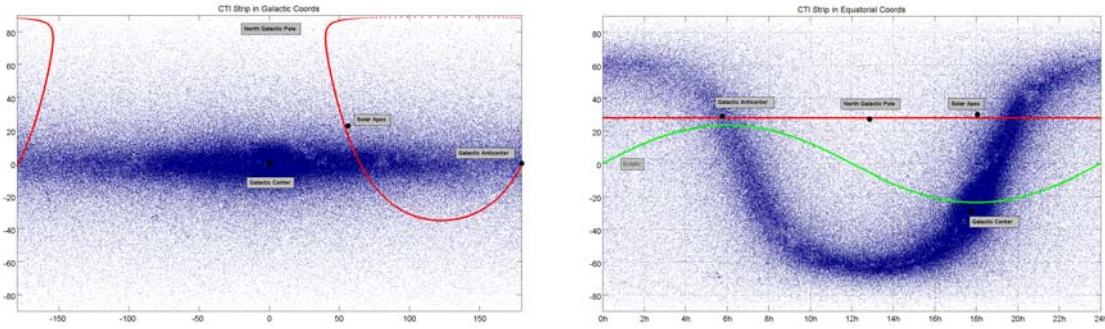


Fig. 13. The left panel (abscissa: Galactic longitude, ordinate: Galactic longitude, both in degrees) shows the distribution of stars observed by CTI-II in Galactic coordinates. The star density in this representation replicates that shown in Fig. 12. The red line shows the one-degree wide CTI-II field of regard traced out in the course of each year of observation. The right panel (abscissa: right ascension in hours, ordinate: declination in degrees) shows the same field of regard but represented in the equatorial coordinate system in which observations are made. The constant declination red line again shows the one-degree wide CTI-II field. The green curve shows the ecliptic along which planets move. Solar system debris above the ecliptic will also be sampled by CTI-II. The plotted points in both panels are the 2MASS 1.2micron (J bandpass) stellar observations for  $12.0 \leq J \leq 12.2$ , thus the data in Fig. 13 and Fig. 12 derive from the same source.

We can estimate the number of stars in the CTI-II field, which will, of course, be a strip on the celestial sphere. Bahcall and Soniera ([16] and references therein) show that in the North Galactic Pole (NGP in Fig. 13, right), we expect more than 500 stars per square degree brighter than  $V = 18$ , the magnitude at which CTI-II observes with a  $S/N \geq 100$ . The CTI-II strip, a complete small circle on the sky, will encompass more than 300 square degrees. Based on star counts from existing catalogs, the CTI-II strip will include more than a million stars brighter than 18<sup>th</sup> magnitude in  $V$ .

Of course, the situation gets better at lower Galactic latitudes because the number of stars per square degree increases dramatically. The situation simultaneously becomes worse as these lower latitudes are sampled, because the density of stars increases so much that crowding becomes a significant effect in two senses. The first is that the probability of having the images of  $V=18$  stars so close together that they are useless as photometric standards increases. An additional effect is that observations become “confusion limited,” which means that the images of stars overlap, and the background light derives from crowded faint stars, not from the night sky background. Of these two effects, the formation of optical doubles tends to be the more important when considering the density of standard stars to be expected in the CTI-II catalog.

The situation is still not simple. To “astrophysical accuracy,” half of the stars in the Galaxy are intrinsically variable. These stars should be rejected as “standard,” because the observed brightness will depend upon when they might be observed. Similarly, half of the stars (including stars that are variables) are in binary or multiple systems. The vast majority of these systems are sufficiently distant that the image of the star will appear as a single seeing-blurred PSF. Binary stars that exhibit variability are not robust standard stars. In addition, space-based telescopes, unhindered by atmospheric seeing, can often resolve these stars, leading to ambiguity (at best) in their use as photometric standard stars.

CTI-II has built into the design of its observing program the ability to discriminate against many variable and binary stars based upon photometry and astrometry. With a predicted three milliarcsecond rms per night astrometric measurement uncertainty, CTI-II will discover unresolved binary stars to a distance of some hundreds of parsecs. Because the focal plane mosaic includes five filter bandpasses observed sequentially with a separation of about one minute of time, most stars will be sampled for short-term variability on this timescale. CTI-II operates every clear night, so stars are sampled routinely at one day intervals for variability characteristic of common variable and unresolved binaries that show extrinsic variability such as pulsating  $\delta$  Cephei stars (cepheids) and RR Lyrae variables, as well as eclipsing variable

stars. While these observing cadences do not fully resolve all possible stellar variability modes, they are sufficient to *detect* variability, thereby ruling the star out as a possible standard star.

The photometric precision we seek is ultimately limited by the brightness of the star as observed by CTI-II. For sufficiently bright stars, photometric uncertainties less than 1% (0.01 magnitude) are expected. Achieving this goal requires care in the design of CTI-II, application of techniques pioneered by others for removing the instrumental signature while calibrating the absolute throughput of the telescope [17, 18], and innovative instrumentation to measure the real-time wavelength dependent extinction of the atmosphere. The suite of instruments supporting the CTI-II observatory is designed to do exactly that.

The strip of standard stars supports the AF mission for space surveillance in multiple ways:

1. It provides a set of many thousands of stars observed to be non-variable and to have no indications of being binary from astrometric measurements.
2. Repeated measurements confirm the measurement and measurement uncertainty of photometric magnitudes and colors and astrometric position.
3. The precision of the repeated measurements is equivalent to space-based photometric and astrometric missions. Spacecraft instruments can be calibrated to this strip, as well as ground-based telescopes.
4. The strip of standards provides both photometric calibration for radiometric purposes, as well as astrometric calibration for FOV and field scale calibration.
5. For ground-based observations the strip is continuously visible at all observable hour angles, thus calibrations can be done at constant airmass.
6. Because the strip is continuously available classical extinction measurements using Langley plots generated with stars both east and west of the meridian can be accomplished.
7. The density of stars is sufficiently great that pointing a telescope with a reasonable FOV (arcminutes or greater) anywhere in the strip will almost certainly provide one or more standard stars.

During the course of this Conference we will hear about several programs that could benefit from having access to this well calibrated strip of sky, including imaging and non-imaging space surveillance systems.

## 5.0 REFERENCES

[1] McGraw, J.T., Angel, J.R.P., and Sargent, T.A., "A CCD Transit-telescope Survey for Galactic and Extragalactic Variability and Polarization," *SPIE Proc. Vol. 264*, p. 20, 1980.

[2] McGraw, J.T., Stockman, H.S., Angel, J.R.P., Epps, H., and Williams, J.T., "The CCD/transit instrument (CTI) deep photometric and polarimetric survey - a progress report," *SPIE Proc. Vol. 331*, p. 137, 1983.

[3] McGraw, J.T., Cawson, M.G.M., Keane, M.J., "Operation of the CCD/Transit Instrument (CTI)," *SPIE Proc. Vol. 627*, p. 60, 1986.

[4] McGraw, J.T., "A Strip Search of the Universe," *Variable Stars and Galaxies, ASP Conference Series*, Vol. 30, p. 77 (San Francisco: Astronomical Society of the Pacific, 1992).

[5] York, D. G. and 144 additional authors, *Astron. J.* **120**, 1579. "The Sloan Digital Sky Survey: Technical Summary."

[6] Mahabal, A., Djorgovski, S. G., Graham, M. and 15 additional authors, AAS Meeting 203, #38.11. "The Palomar-Quest Synoptic Sky Survey."

[7] Stone, R. C., Monet, D. G., Monet, A. K. B., Walker, R. L. and Ables, H. D. 1996, *Astron. J.* **111**, 1721. "The Flagstaff Astrometric Scanning Transit Telescope (FASTT) and Star Positions Determined in the Extragalactic Reference Frame."

[8] Evans, D. W., Irwin, M. J. and Helmer, L. 2002, *Astron. Astrophys.* **395**, 347. “The Carlsberg Meridian Telescope CCD drift scan survey.”

[9] [http://www.lsst.org/About/optical\\_design.shtml](http://www.lsst.org/About/optical_design.shtml) and linked references.

[10] Ackermann, M. R., McGraw, J. T., Zimmer, P. C., and Williams, Tom 2006, *Proceedings of the 2006 AMOS Conference*, “The Unique Optical Design of the NESSI Survey Telescope.”

[11] Dawsey, M., Gimmestad, G., Roberts, D., McGraw, J. T., Zimmer, P. and Fitch, J. 2006, *Proc. Soc. Photo-opt. Inst. Eng.* **6270**, 62701F. “LIDAR for Measuring Atmospheric Extinction.”

[12] Zimmer, P. C., McGraw, J. T., Gimmestad, G., Roberts, D., Stewart, J., Dawsey, M., Fitch, J., Smith, J., Townsend, A. and Black, B. 2006, *American Astronomical Society Meeting 209, BAAS* **38**, 1109. “ALE: Astronomical Lidar for Extinction.”

[13] Pier, J. R., Munn, J. A., Hindsley, R. B., Hennessy, G. S., Kent, S. M., Lupton, R. H. and Ivezić, Z. 2003, *Astron. J.* **125**, 1559. “Astrometric Calibration of the Sloan Digital Sky Survey.”

[14] Kolmogorov, A. N. 1941, *Dokl. Akad. Navk SSR*, Vol. 30, p. 301. “The Local Structure of Turbulence in Incompressible Viscous Fluid for Very Large Reynolds Number.”

[15] Tatarski, V. I. 1961, “Wave Propagation in a Turbulent Medium,” (McGraw-Hill, NY), Translated by R. A. Silverman.

[16] Bahcall, J. N. and Soniera, R. M. 1984, *ApJ Supplement*, 55, 67, “Comparisons of a Standard Galaxy Model with Stellar Observations in Five Fields.”

[17] Stubbs, C. W. and Tonry, J. L. 2006, *Astron. J.* 246, 1436. “Toward 1% Photometry: End-to-End Calibration of Astronomical Telescopes and Detectors.”

[18] Stubbs, C. W., Slater, S. K., Yorke, J. B. Sherman, D., Smith, R. C., Suntzeff, N., Saha, A., Tonry, J. L., Masiero, J. and Rodney, S. 2007, *ASP Conf. Series*, Ed. C. Sterken, **364**, 373. “Preliminary Results from Detector-Based Throughput Calibration of the CTIO Mosaic Imager and Blanco Telescope Using a Tunable Laser.”